THE PLASTIC DEFORMATION OF LONG RANGE ORDERED 18R MARTENSITIC SINGLE CRYSTALS OF Cu-Zn-Al ALLOYS

I. Macroscopic Properties

A. Cuniberti[+], R. Romero[+] and M. Ahlers[*]

[+]IFIMAT, Facultad de Ciencias Exactas, Universidad Nacional del Centro de la Provincia de Buenos Aires, Pinto 399, 7000 Tandil, Argentina

[*]Centro Atómico Bariloche, 8400 S.C. de Bariloche, Argentina

Abstract

Single crystals of 18R martensite, which were stress induced by compression from β phase single crystals, were deformed in compression at room temperature. Irreversible slip was observed, which was retained after unloading and after retransforming to the β phase. The slip line markings were analyzed and it was found that they correspond to slip on the basal plane of the 18R structure, with the ordinary Burgers vector parallel to the close packed direction consisting of copper atoms. The critical resolved shear stress was determined as (77 ± 11) MPa. It is independent of the degree of $L1_2$ order that can be quenched-in in the high temperature β phase, but depends on the stabilization in the martensite. The results are analyzed in terms of the deformation mechanisms which are commonly observed in long range ordered close packed lattices based on the fcc structure.

1. Introduction

The plastic behaviour of long range ordered alloys based on the fcc lattice has found considerable interest due to the favourable high temperature properties of the superalloys (for reviews see: Koch et al. eds., 1985). In many of these ordered alloys the critical stress increases with increasing temperature. This has been found for alloys with the Cu_3Au-type $L1_2$ structure, among them Ni_3Al, but also for alloys with the CuAu-type $L1_0$ structure, as AlTi (Kawabata et al., 1985, 1990). Whereas the Cu_3Au structure remains cubic on ordering, long range order in the $L1_0$ structure is associated with a tetragonal distortion of the originally cubic lattice. If the ordering occurs below the melting point of the alloy, this leads to the formation of {110} twins in the single crystals (Pashley et al., 1969). Only if the ordering energy is so high that the alloy is ordered at the melting point, can a twin free single crystal be grown (Kawabata et al., 1985).

Single crystals of an ordered close packed structure can also be obtained by a martensitic transformation in many shape memory alloys (see: Warlimont and Delaey, 1974, Ahlers, 1986). The ordered B2 or $L2_1$ high temperature β phase is transformed to close packed structures which inherit the atom distribution due to the diffusionless nature of the transformation. The most commonly observed structures differ by the stacking sequence of the close packed planes. In the binary Cu-Zn and ternary Cu-Zn based alloys one finds the 3R ABCABC fct structure with $L1_0$ order at the low end of the electron concentrations for which the β phase is stable at high temperatures. If $L2_1$ order is inherited, instead, the 6R

structure is induced. At intermediate e/a a 9R (or 18R) ABCBCACAB orthorhombic structure is found, and at high e/a the martensite is hexagonal, 2H, or has a slightly distorted, orthorhombic structure.

In figure 1 are shown four unit cells of the high temperature $L2_1$ structure, and the corresponding 6R martensite lattice after the transformation, with a tetragonal cell. In addition to the tetragonal axes system, denoted by the index t, the orthorhombic axes system is also used, indicated by o. The 18R and 2H structures can formally be derived from 6R by adding stacking faults on each third and second plane, respectively. (Due to the tetragonality, the $[001]_o$ axis of 18R is slightly inclined with respect to $[100]_o$, therefore the structure is monoclinic, in fact.) By applying external stresses the three structures can be transformed into each other for a given β phase single crystal (Ahlers, 1986). It is therefore possible to study the plastic behaviour of the three structures separately for the same alloy.

The positive temperature dependence of the critical resolved shear stress for plastic deformation in $L1_2$ structures has been ascribed to the cross slip of superdislocations by the Kear-Wilsdorf mechanism. In $L1_0$ ordered alloys this mechanism should be absent when slip occurs with a Burgers vector that is parallel to $[010]_o$ (figure 1). Nevertheless, in TiAl with this structure one finds also a positive temperature dependence of the CRSS (Kawabata et al., 1985). Whether the same occurs in some of the close packed martensitic phases with a smaller ordering energy, has not been investigated so far. Since, however, the martensite retransforms to the high temperature β phase at A_s, the

measurement of the temperature dependence of the CRSS requires a special treatment to make sure that the CRSS remains reliable. In this first report the mechanical properties of 18R martensite single crystals at room temperature are presented. In a second paper, the corresponding observations by TEM are communicated (Rodriguez et al, 1991). Further measurements on the temperature and structure dependence of the CRSS will be reserved for a future paper.

2. Experimental procedure

The Cu-Zn-Al alloys were prepared in quartz capsules under argon atmosphere, starting with 5N pure metals. The alloy compositions and the measured transformation temperatures M_s on cooling are given in table 1. All of them have an electron concentration e/a = 1.48, corresponding to the maximum stability of the β phase.

Table 1

Alloy No.	at% Cu	at% Zn	at% Al	measured M_s [K]
1	69.52	12.96	17.52	316
2	69.92	12.16	17.92	336
3	68.40	15.14	16.43	261

The β phase single crystals were grown by the Bridgman method in closed quartz tubes in a temperature gradient of 1 K mm^{-1} with a growth velocity of 30 mm/h. They remained for several hours at a homogeneization temperature close to the melting point. The crystals were spark machined into cylindrical samples of 11 mm

length and 4 mm diameter for the compression tests. The orientations of the single crystals were determined in the high temperature β phase.

In order to obtain a martensitic single crystal from the alloys with an M_s above room temperature, the following procedure was adopted: The crystal was heated for 5 min to 1070 K and then quenched into water at 350K. At this temperatue the sample was compressed until the whole crystal had transformed martensitically to the 18R structure. After cooling under stress the martensite was retained at room temperature. By optical microscopy with polarized light and by X-ray analysis it was made sure that the whole crystal consisted of a single variant martensite phase. Due to the transformation, the cylindrical crystal had changed its shape and the end faces were no longer normal to the sample axis. This was rectified by an additional mechanical grinding of the sample ends to right angles. For surface observations the samples were electropolished at 273 to 278 K in a solution of 10% HNO_3 in CH_3OH. All deformation experiments were done in compression in an Instron 1123 machine at a strain rate of $7.6.10^{-4}$ s^{-1}. In order to reduce the stress inhomogeneities along the sample during the deformation, the end faces were covered with a thin teflon film and lubricated with grease.

The orientation of the martensite variant which is stress induced is determined by the crystal axis in the β phase. For the samples which were martensitic at room temperature, it was verified in all cases by X-rays that the expected martensite variant is indeed induced. Although, in general, an orientation determination of the 18R martensite is difficult due to the large

number of Laue spots, in this case the approximate orientation was already known from the relationship with the β phase, and therefore the orientation of the sample axis and some additional surface markings could easily be determined by X-rays. In this way all surface traces could be analyzed with respect to the particular martensitie variant.

3. Experimental results

In figure 2 are shown the orientations of the compression axes in the high temperature β phase of the alloys 1 and 2 of table 1, which are martensitic at room temperature. In the stereographic projection of figure 3 are plotted, with reference to the β phase lattice, and locating the compression axes inside the unit standard triangle C, the following quantities (by crosses): The habit plane normal $\underline{P}'_1$ of the most favourable variant, the martensite shear direction, $\underline{d}'_1$, the normal of the basal plane $\underline{P}_2$ at $(001)_o$ of the orthorhombic lattice, and the $[100]_o$ and $[010]_o$ directions corresponding to those of figure 1. The orientation of the Bain axis, parallel to $[001]_\beta$, which transforms to the tetragonal axis in the 6R structure (see figure 1), is also marked (by BC). The orientation relationship between β and the martensite is that calculated for a martensitic transformation without volume change and a tetragonal distortion of the fct basic 6R lattice of $(c/a)_{fct} = 0.94$. The martensite variant that is shown is that with the highest Schmid factor, which indeed has been observed to be induced. It should be remarked here, that stressing the martensitic single crystal in a direction that lies outside the unit triangle, for example after

cutting from the martensitic single crystal a sample with inclined axes a different martensite variant is induced, instead of deforming plastically the original one.. This limits considerably the axis orientations, for which deformation studies can be made in the martensitic state.

In figure 4 is shown a typical stress-strain curve for an 18R martensitic single crystal deformed in compression at 295K with a strain rate of $\varepsilon = 7.6.10^{-4}\ s^{-1}$. A smooth transition from the elastic to the plastic range with neither a yield point nor serrations is typical for the plasticity of these alloys at room temperature with the exception of axes less than 18° away from $[010]_\beta$, for which a load drop after the start of plastic deformation is observed.

The surface of a martensitic single crystal deformed to $\varepsilon = 3\%$ is reproduced in the foto of figure 5. As can be seen here and as is generally observed, the crystal is covered mainly with one type of parallel markings, which can be followed around all the circumference of the cylindrical crystal. They disappear when the shear vector lies in the surface. Some additional well marked lines inclined to the main shear system have also been observed. They are seen, however, only in a part of the crystal surface. In the following they will be denoted by $\{\bar{1}28\}_0$, the reason for it will be given below.

By a multiple surface analysis the orientations of the planes of the deformation traces and of the corresponding shear directions were determined with respect to the orthorhombic axes $[100]_0$, $[010]_0$ and the plane normal $(001)_0$ (since due to the monoclinic distortion the $[001]_0$ direction deviates by about 2°

from the normal of the $(001)_0$ basal plane) The results are plotted in figure 6. They show that the shear plane is the basal plane, and that the shear direction is parallel to $[010]_0$. The second set of deformation traces has the plane close to $\underline{P}_0$ and $\underline{P}'_0$. These planes lie near the $(1\bar{2}8)_0$ and $(128)_0$ planes of the 18R martensite, and for this reason were denoted by the term "$\{\bar{1}28\}_0$ shear". (The $1\bar{2}8)_0$ and $(128)_0$ planes are not shown in the figure, they are close to $\underline{P}'_1$ and $\underline{d}'_1$). The shear direction $\underline{d}_0$ and $\underline{d}'_0$ of the $\{128\}_0$ shear could not be well determined. The possible range is indicated by a broken line, corresponding to the range for which the surface upheaval disappears. The centre of the range points to displacements parallel to the Burgers vector of the superdislocaions (denoted by a filled triangle).

On the basis of the trace analysis, the shear system is established to be the $(001)_0$ $[010]_0$ system. Its critical resolved shear stress (CRSS) τ_d has been determined and is plotted in figure 7 as a function of the Schmid factor. The scatter is large, but no systematic orientation dependence is found from which it is concluded that within the experimental error the Schmid law is obeyed for all orientations analyzed. The scatter in the experimental data can be accounted for by the uncertainty in the determination of the crystal orientation and the crystal diameter. the numerical value for the critial resolved shear stress for $(001)_0$ $[010]_0$ slip is

$$\tau_d = (77 \pm 11) \text{ MPa}$$

Several β phase single crystals of composition 3 (table 1)

were also deformed at room temperature in the high temperature phase. A typical stress-strain curve is shown in figure 8. At a critical stress σ_M a single variant 18R martensite is started to be induced in compression. On its completion the plastic deformation starts at σ_d. On unloading, the retransformation to β occurs, but a remanent plastic deformation ε_β is retained. A detailed analysis shows that the plastic strain in the martensite, ε_M, is nearly equal to that remaining in the β phase, ε_β. Also the hysteresis between the stress to induce the martensite and the retransformation stress to the β phase has increased, compared to the undeformed samples. After unloading the sample is again in the β phase. No indication for retained martensite could be obtained, neither by polarized optical microscopy nor by X-ray analysis. The critical resolved shear stress for plastic deformation is the same as for the alloys which are martensitic at room temperature, at least within the experimental scatter. Since the whole crystal transforms to a single variant in applying the stress, the sample axis becomes inclined to the stress axis without changing the β phase orientation. Therefore the Schmid factor can be calculated with respect to the original β phase orientation, and not with respect to a displaced axis. It may be mentioned, however, that the differences in the Schmid factor lead to changes in τ_d which remains within the scatter of the data.

It is well known that heat treatments in the β phase (Rapacioli and Ahlers, 1977, 1979) and in the martensite (Abu Arab and Ahlers, 1988) modify the properties. Of special interest in the present context is the quenching treatment in the high temperature β phase prior to the deformation. A quenching from

above the long range order temperature of $L2_1$, or B2 order introduces a high density of antiphase domain boundaries (Rapacioli and Ahlers, 1977). By a quenching from below about 550K, the corresponding incomplete $L2_1$ order can be quenched in (Planes et al., 1990). Quenching from intermediate temperatures can also lead to the precipitation of γ-particles (Rapacioli et al, 1981). The influence of these modifications on the critical resolved shear stress has been studied by quenching crystals of alloy 3 (table 1) from different temperatures, and immediately transforming and deforming the single crystals. The crystals were cooled in air from 1073 K, with a thermocouple attached to them. When the required quench temperature T_Q was reached, the samples were quenched into iced water. After the stress inducing of the martensite, the deformation leads to the activation of the same $(001)_0$ $[010]_0$ system observed before. The critical resolved shear stress τ_d is shown as a function of the quench temperature T_Q in figure 9. The corresponding β phase orientations are shown in the unit triangle. The CRSS τ_d shows a remarkably small variation with T_Q: there may be a small increase of τ_α with T_Q, but the scatter is too large to affirm this with certainty. The ordering temperatures for $L2_1$ and B2 order are taken from the paper by Rapacioli and Ahlers (1977), they had been measured for the same electron concentrations.

When, after quenching, the martensitic single crystal is annealed at sufficiently high temperatures, which already include room temperature, diffusion controlled changes occur which lead to an increase in the retransformation temperature. This stabilization had been studied in detail for alloys similar to the

present ones (Abu Arab and Ahlers, 1988). The influence of stabilization on the CRSS has been analyzed using single crystals of alloy 3 (table 1) with orientation C(Δ) of figure 9. These crystals were cooled slowly in air from 1073 K to 573 K and then were quenched into iced water. A martensitic single crystal was induced at 315 K, and aged under stress for 10^5 s at this temperature. This procedure is known to lead to a saturation stabilization. The crystal was then cooled to room temperature, and deformed plastically at this temperature. Again, deformation on the $(001)_0$ $[010]_0$ system was induced. However, the critial resolved shear stress had increased to (103 ± 2) MPa after stabilization.

4. Discussion

In long range ordered alloys based on the face centered cubic lattice, several deformation mechanisms have been observed (see several papers in: Koch et al., eds., 1985). They will now be discussed with reference to the martensitic 18R single crystals. The 18R structure differs from the fcc lattice only by a different stacking sequence of the basal planes. Since the principal slip occurs on the basal plane of 18R, close correlations of the deformation behavior between both structures can be expected. It is clear however that the $\{128\}_0$ deformation traces have no relationship with the fct lattices. Here the stacking sequence is important. From figure 6 can be seen that the two $\{128\}_0$ shear systems $\underline{P}_0$, $\underline{d}_0$ and $\underline{p}'_0$, $\underline{d}'_0$ are equivalent with respect to the orthorhombic axes system. The plane $\underline{P}_0$ is nearly parallel to the habit plane $\underline{P}_1$, but the direction $\underline{d}_0$ is not parallel to the

martensitic shear direction $\underline{d}'_1$. The two systems $\underline{P}_0$, $\underline{d}_0$ and $\underline{P}'_0$, $\underline{d}'_0$ are not equivalent with respect to the compression axes. Whereas the absolute value of the Schmid factor is favourable for $\underline{P}_0$, $\underline{d}_0$, it is very small for the $\underline{P}'_0$, $\underline{d}'_0$ system, as can be guessed from a simple inspection of figure 6. No systematic dependence on the axis orientation is found, since only few $\{128\}_0$ markings are observed, if ever. In addition no changes in the stress-strain curves associated with the formation of the $\{128\}_0$ traces are found. It is therefore concluded that this shear system is activated only accidentally. In martensite obtained by cooling $\{128\}_0$ defects have been analyzed in detail by Andrade et al. (1982), who found by TEM that the $\{128\}_0$ faults ended in basal plane faults. However, a $(\underline{p}_0, \underline{d}_0)$ shear system has not been obsered before, and it is not clear on what mechanism it is based.

The basal plane slip will now be discussed with reference to figure 10, which shows the basic fct 6R cell, with the four different sublattices inherited from the high temperature β phase. Sublattices I and II are occupied mainly by Cu-atoms. For a B2 inherited structure sublattices III and IV are occupied with the same probability by the rest of the atoms, leading to an $L1_0$ unit cell. In this cell the three shortest translation Burgers vectors are according to increasing length: $\frac{b_0}{2}[010]_0$, $[a_0, \pm \frac{b_0}{2}, 0]_0$ and $a_0[100]_0$. For an inherited $L2_1$ order, sublattices III and IV are occupied with different probabilities, and the translation vectors are twice as large as before, except $a_0[100]_0$ which remains the same, and now becomes the shortest translational Burgers vector.

The feasability of the slip with the three different Burgers vectors can be evaluated by comparing the Schmid factors. For the

compression axes in the unit triangle C of figure 6, the most favourable shear system is the observed $(001)_0$ $[010]_0$. Only at the $<110>\beta$ corner of the unit triangle becomes the slip with the Burgers vector $[a_0, -\frac{b_0}{2}, 0]_0$ equally favourable (This Burgers vector is denoted by SD in figure 6). The Schmid factor is extremely unfavourable for the $[100]_0$ $(001)_0$ shear system. If we take also into consideration that the quenching temperature has little effect on τ_d, which implies that $L2_1$ order does not affect critically the CRSS, the observation of the $[010]_0(001)_0$ slip system is not unreasonable. Since it is not possible to move the axes outside the unit triangle C, as has been discussed above, the critical stresses for the other slip systems cannot be determined experimentally.

It is interesting to compare the CRSS measured in the present Cu-Zn-Al alloys at an electron concentration of e/a = 1.48 with a value obtained for a Cu-39.6at% Zn single crystal deformed in compression at 143K, above M_s (Arneodo and Ahlers, 1973). From the measured stress σ = 200 MPa and a Schmid factor of 0.357 a resolved shear stress of 71 MPa is deduced, close to the values obtained for the present alloys. If we consider a splitting of the $[010]_0$ ordinary dislocation into two partials, a stacking fault is created which involves also local changes in long range B2 inherited order. If the stacking fault plays a role in the mobility of the dislocation, then it may be argued that since the B2 ordering temperature changes little with composition, so does the critical stress τ_d. However, that this is not the only factor in determining τ_d is evident from the observation that after the stabilization of the martensite the CRSS τ_d has increased by 30%.

It is known that, although the degree of long range order changes little on stabilization (Hashiguchi et al., 1986), the tetragonal distortion is modified considerably (Delaey et al., 1984). It is therefore most likely that, depending on the local atom configuration elastic dipoles or multipoles exist, which interact strongly with the moving dislocations. A third contribution to τ_d possibly arises from the interaction of the dislocations with the {128} type faults, as will be discussed in the subsequent paper (Rodriguez et al., (1991)).

5. Conclusions

Martensitic 18R single crystals of Cu-Zn-Al alloys were deformed plastically in compression at room temperature.

In addition to some accidental traces with planes close to $\{128\}_0$, the plastic deformation occurred mainly by a shear on the $(001)_0$ basal plane, with the shear direction parallel to the ordinary $[010]_0$ Burges vector, which is the shortest and the most favoured one by its Schmid factor in an $L1_0$ ordered lattice.

The critical stress is τ_d = (77±11) M Pa. It depends little on small changes in the degree of long range order retained after quenching from higher temperatures. However, a strong influence of the stabilization in the martensite is found. From this it is concluded that local lattice distortions due to the long range order, like elastic dipoles, constitute an important contribution to the critical resolved shear stress for the plastic deformation of 18R martensitic single crystals.

References

Abu Arab, A. and M. Ahlers, 1988, Acta Met. 27, 2627.

Ahlers, M., 1986, Progr. Mat. Sci. 30, 135.

Andrade, M., L. Delaey and M. Chandrasekaran, 1982, J. de Physique 43, C4 673.

Arneodo, W. and M. Ahlers, 1973, Scripta Met. 7, 1287.

Barceló, G., M. Ahlers and R. Rapacioli, 1977, Zeitschr. Metallkde 70, 732.

Delaey, L., T. Suzuki, J. Van Humbeeck, 1984, Scripta Met. 18, 899.

Hashiguchi, Y., H. Higuchi, I. Matsui, T. Niitani, H. Tokunoh, Y. Ikai, 1986, Proc. Int. Conf. Mat. Transf., Japan Int. Metals, p. 832.

Kawabata, T.K., T. Kanai and O. Izumi, 1985, Acta Metall. 33, 1355.

Kawabata, T.K., T. Abuniya, T. Kanai, O. Izumi, 1990, Acta Metall. et Mater. 38, 1381.

Koch, C.C., C.T. Liu, N.S. Stoloff, eds., 1985, High temperature ordered intermetallic alloys, MRS vol. 39, Pittsburgh, Pa.

Pashley, D.W., J.L. Robertson, M.J. Stowell, 1969, Phil. Mag. 19, 83.

Planes, A., R. Romero and M. Ahlers, 1990, Acta Metall. et Mater. 38, 757.

Rapacioli, R. and M. Ahlers, 1977, Scripta Met, 11, 1147.

Rapacioli, R. and M. Ahlers, 1979, Acta Met. 27, 77.

Rapacioli, R., M. Chandrasekaran, F.c. Lovey, 1981, Proc. Conf. on Solid Solid Phase Transformation, Pittsburgh p.739.

Rodriguez, P.L., A. Cuniberti, R. Romero and F.C. Lovey, 1991, Submitted to Phil. Mag. A.

Warlimont, H. and L. Delaey, 1974, Progr. Mat. Sci. 18, 1.

Figure Captions

Fig. 1 left: The high temperature $L2_1$ structure: 4 elemental cells are shown, with a tetragonal cell delineated in the interior, which transforms martensitically to the 6R tetragonal cell (right). The tetragonal axes system denoted by t. The basal plane of the 6R is also shown, with the axes given in the orthorhombic system, denoted by O. In the $[001]_t$ direction, layers consisting of Cu-atoms (for alloys with Cu concentration > 50%) alternate with those consisting of Cu, Zn and Al in an ordered fashion if $L2_1$ order is inherited, and in a disordered manner for a B2 ordered high temperature phase.

Fig. 2: Orientations of the sample axes within the unit stereographic triangle of the β phase for alloy 1(*, ∇, O) and alloy 2 (+, □, Δ).

Fig. 3: Stereographic projection of the orientation relationship for the most favourable martensite variant induced by a compression with the axis within the triangle denoted by C. Habit plane ($\underline{P}_1'$), martensite shear direction ($\underline{d}_1'$), basal plane $\underline{P}_2$ and the orthorhombic unit axes, as defined in figure 1, all with respect to the β phase orientation. BC the orientation of the Bain axis.

Fig. 4: Stress-strain curve for plastic deformation of an 18R single crystal at 295 K with $\dot{\varepsilon} = 3.10^{-4}\ s^{-1}$. Axis orientation in the β phase given in the unit triangle. Critical stress σ_d

defined as the intersection of the linear elastic and plastic ranges.

Fig. 5: Optical micrograph of the deformation traces of the martensitic single crystal. In addition to the main traces, some isolated bands denoted by $\{128\}_0$ are seen.

Fig. 6: Results of the slip trace analysis plotted in the stereographic projection with respect to the orthorhombic axes system $[100]_0$, $[010]_0$ and the plane normal $(001)_0$. The filled squares (■) are the <100> directions of the bcc phase, and the unit triangle is denoted by C, with the orientations of the sample axes before the transformations. The symbols of the trace analysis coincide with those in the triangle C and with that of figure 2. The main shear planes and directions are denoted by $\underline{P}_{-1}$ and $\underline{d}_{-1}$, respectively. The habit plane is at $\underline{P}'_{-1}$ and the martensite shear has direction $\underline{d}'_{-1}$ (filled circles). The poles of the $\{\bar{1}28\}_0$ type slip planes are denoted by $\underline{P}_{-0}$ and $\underline{P}'_{-0}$. They are close to the $(1\bar{2}8)_0$ and $(128)_0$ planes, respectively. The corresponding directions are denoted by $\underline{d}_{-0}$ and $\underline{d}'_{-0}$, lying within the range given by the broken lines.

Fig. 7: The critical resolved shear stress τ_d for $(001)_0$ $[010]_0$ slip as a function of the Schmid orientation factor μ for the crystal orientations of figure 2.

Fig. 8: Transformation and deformation cycle starting with a β phase single crystal. At σ_M start of the martensitic

transformation. At σ_d start of the plastic deformation of the martensite. Orientation given in the unit triangle (alloy 3 of table 1).

Fig. 9: The influence of quenching from T_Q in the β phase on the CRSS τ_d. Orientations are given in the unit triangle. Ordering temperatures for $L2_1$ and B2 order are also given, according to Rapacioli and Ahlers, 1977 (alloy 3 of table 1).

Fig. 10: The unit cell of the fct 6R ordered lattice inherited from $L2_1$ order in the high temperature β phase. Sublattices I and II occupied by Cu-atoms. Several directions with respect to the fct lattice (denoted t), and the orthorhombic axes system (O) are given.

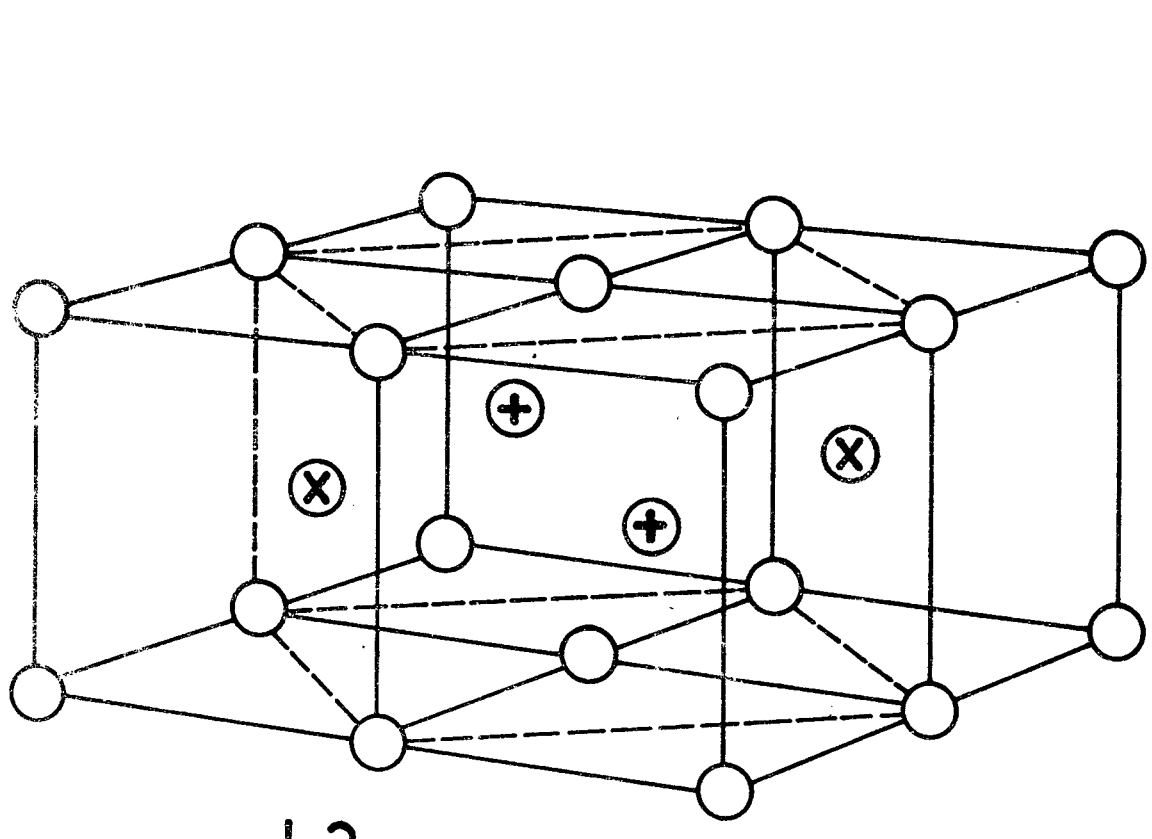

$L2_1$

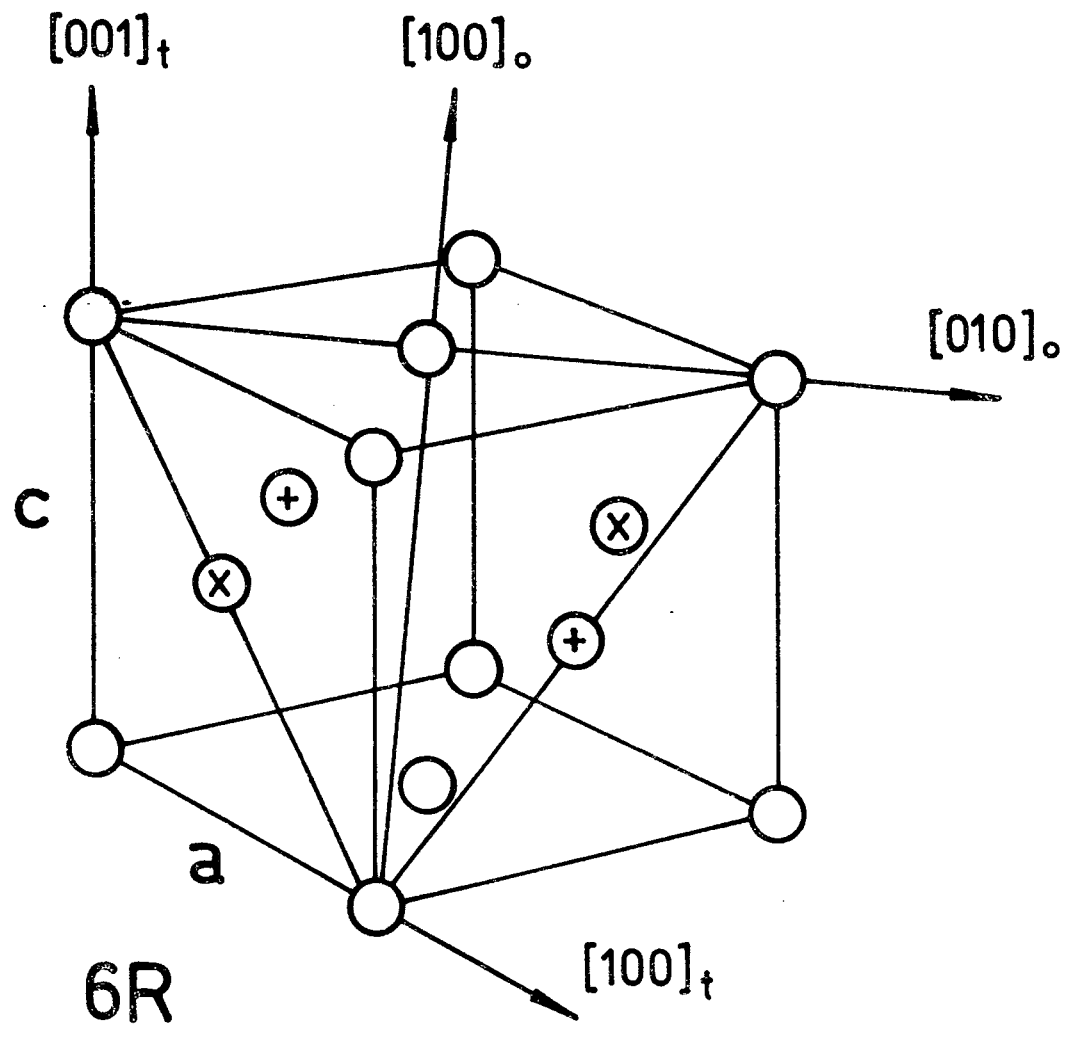

6R

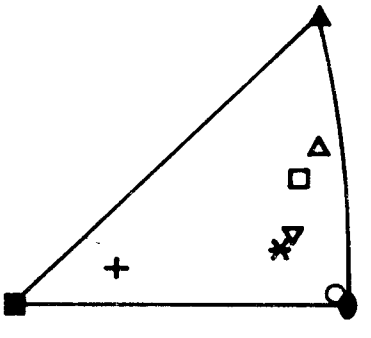

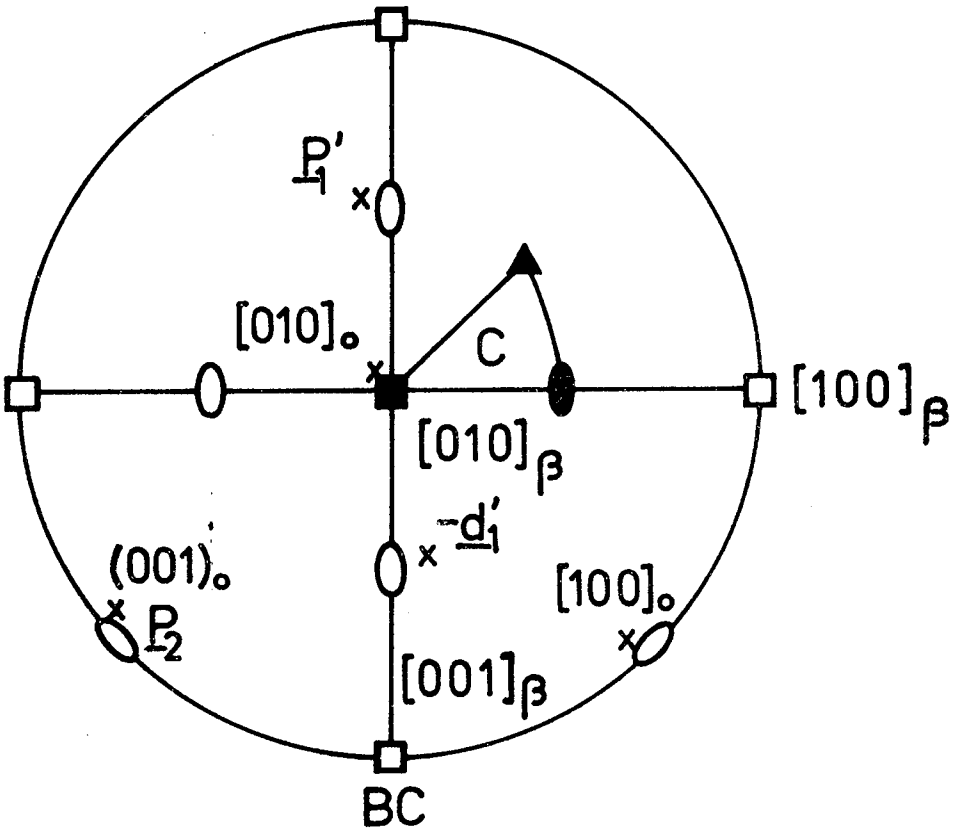
P_1'
$[010]_o$
C
$[100]_\beta$
$[010]_\beta$
$-d_1'$
$(001)_o$
P_2
$[100]_o$
$[001]_\beta$
BC

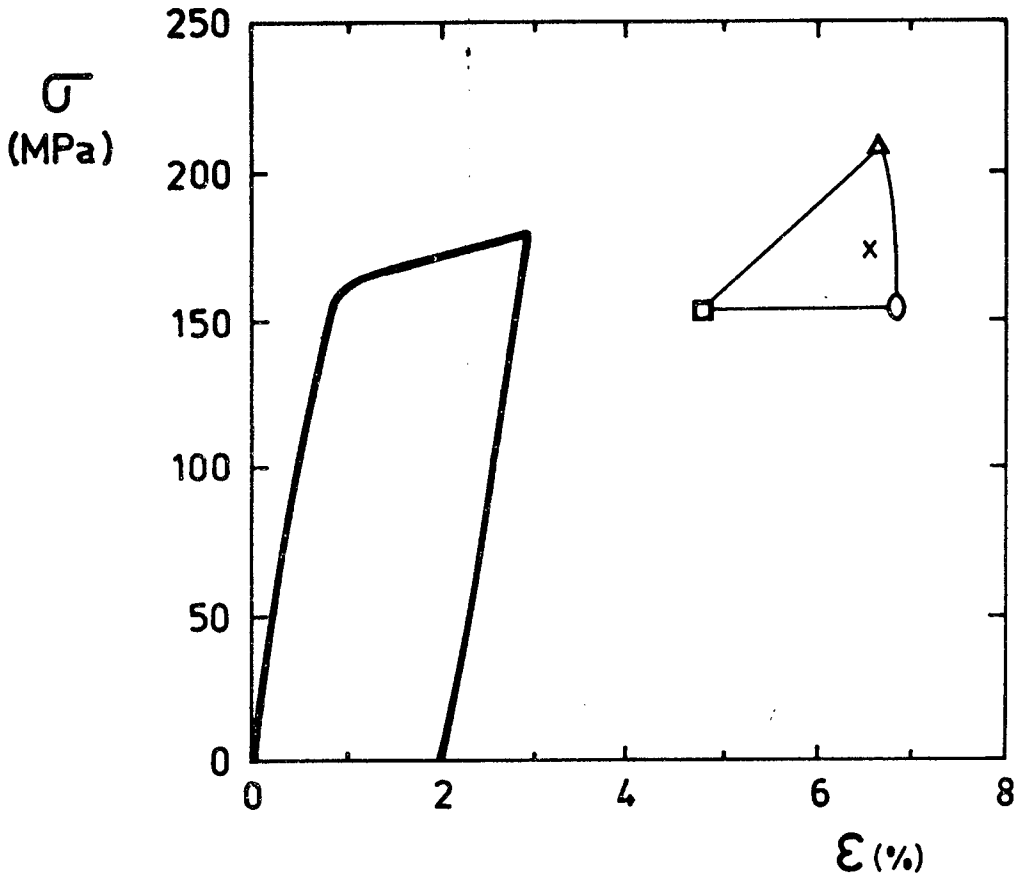
σ̄
(MPa)
250
200
150
100
50
0
0
2
4
6
8
ε (%)
x

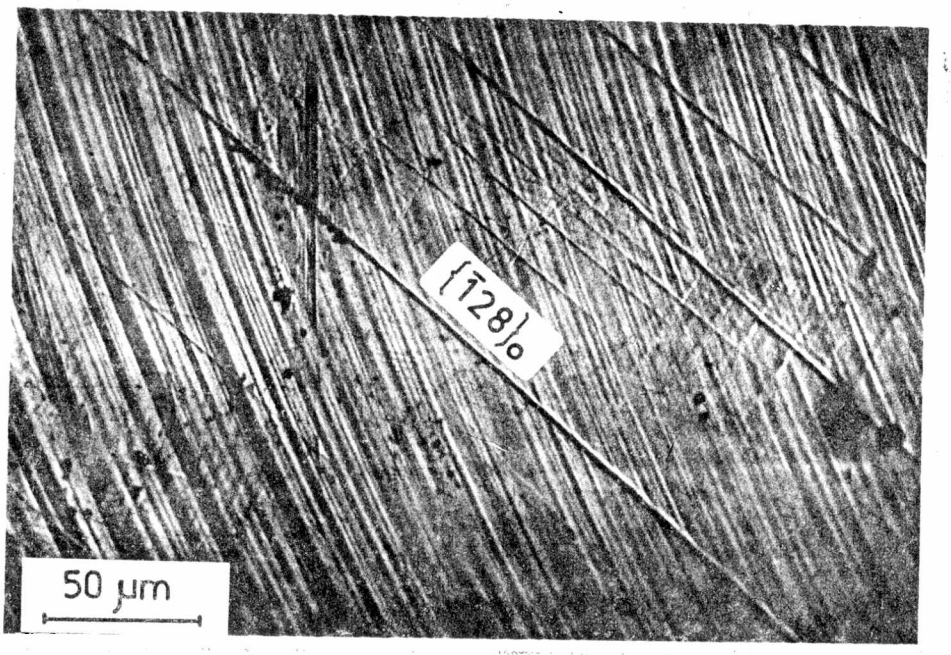
{1̄28}o
50 µm

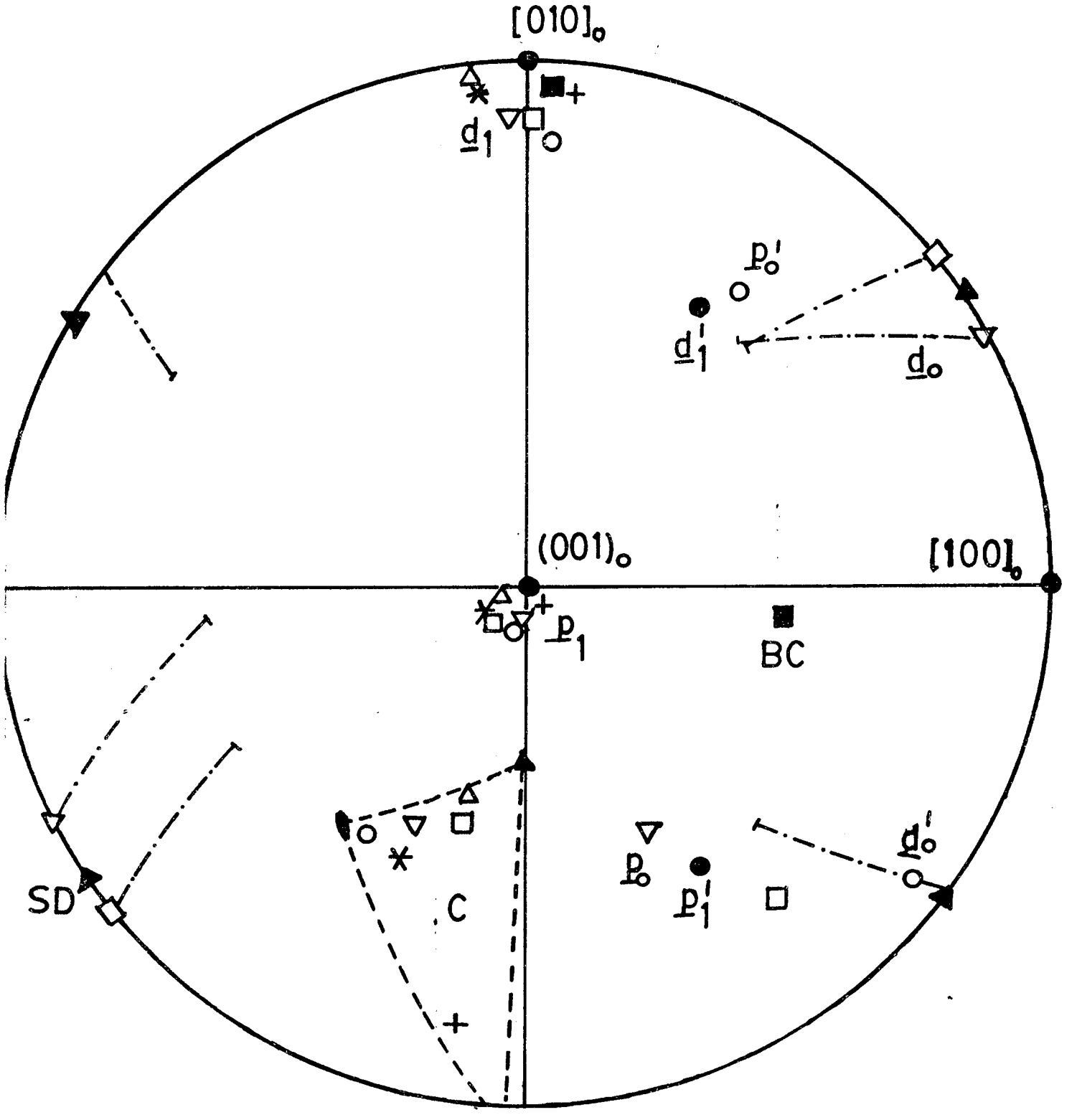
[010]o
d1
p'o
d'1
do
(001)o
[100]o
p1
BC
SD
C
po
p'1
d'o

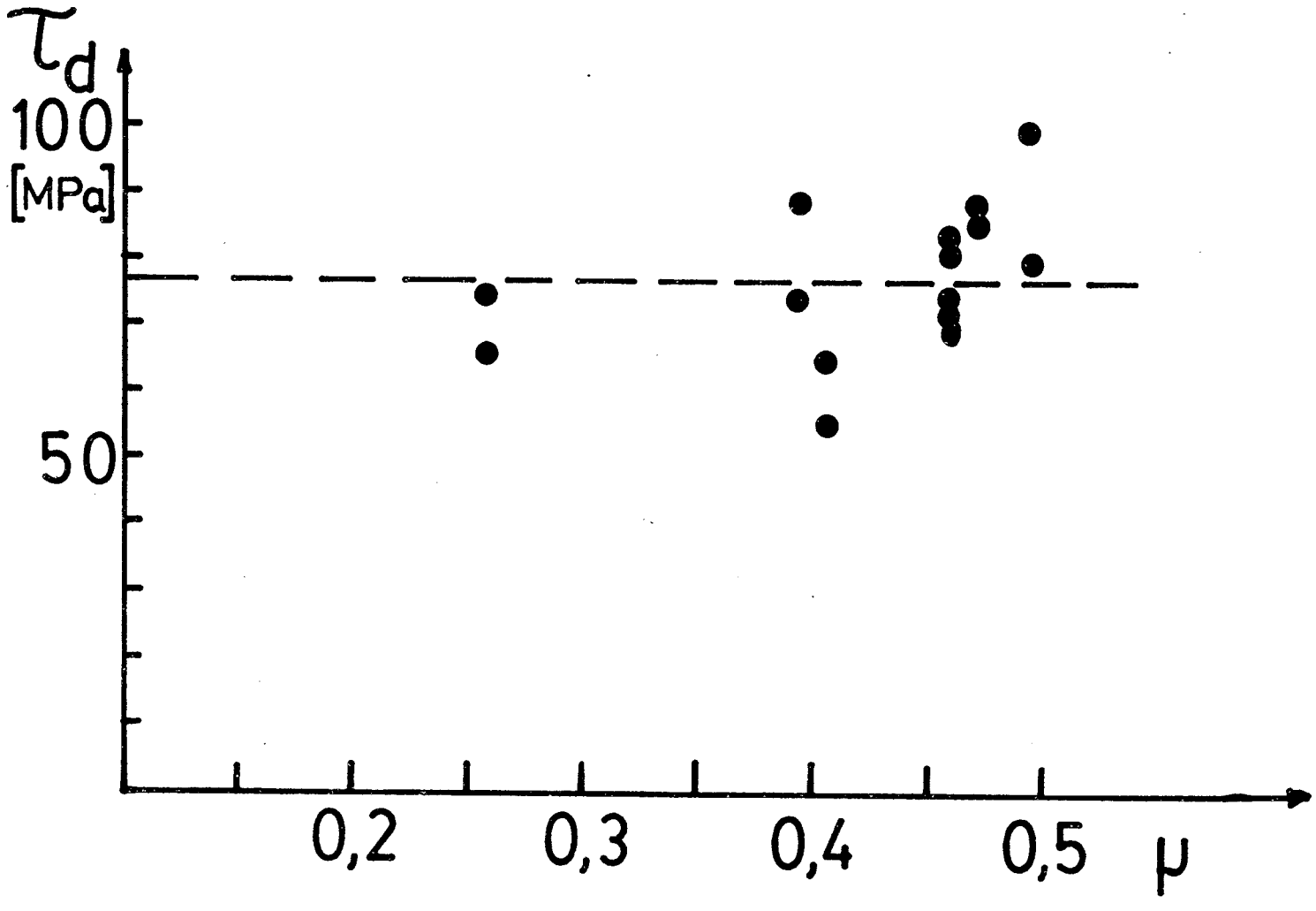
τ_d
100
[MPa]
50
0,2
0,3
0,4
0,5
μ

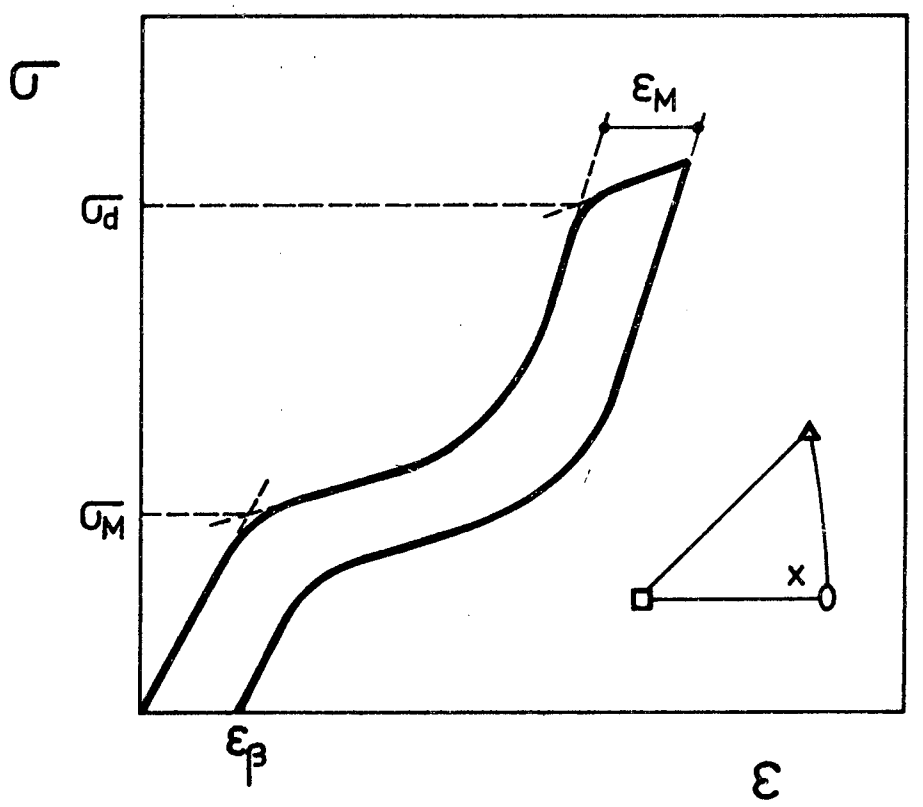
σ
ε_M
σ_d
σ_M
x
ε_β
ε

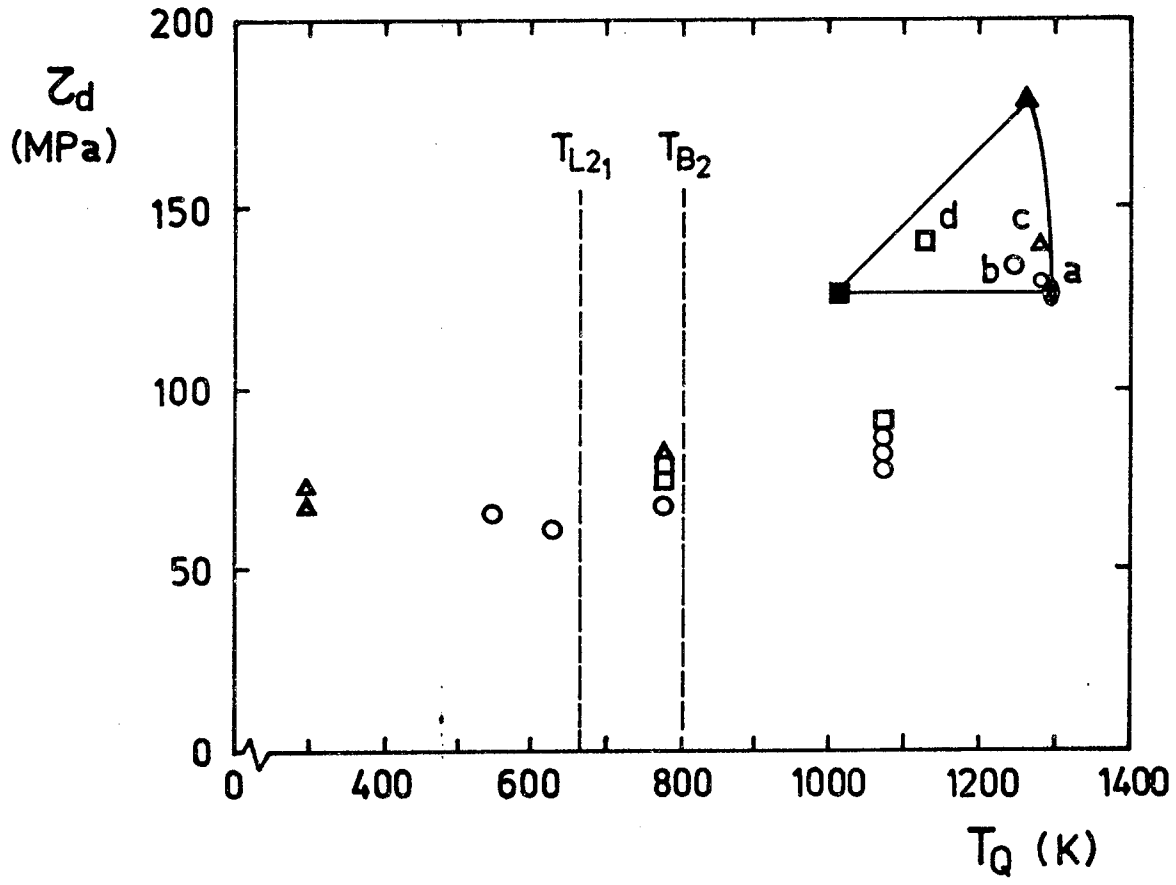
200
150
100
50
0
τ_d
(MPa)
T_{L2_1}
T_{B_2}
d
c
b
a
0
400
600
800
1000
1200
1400
T_Q (K)

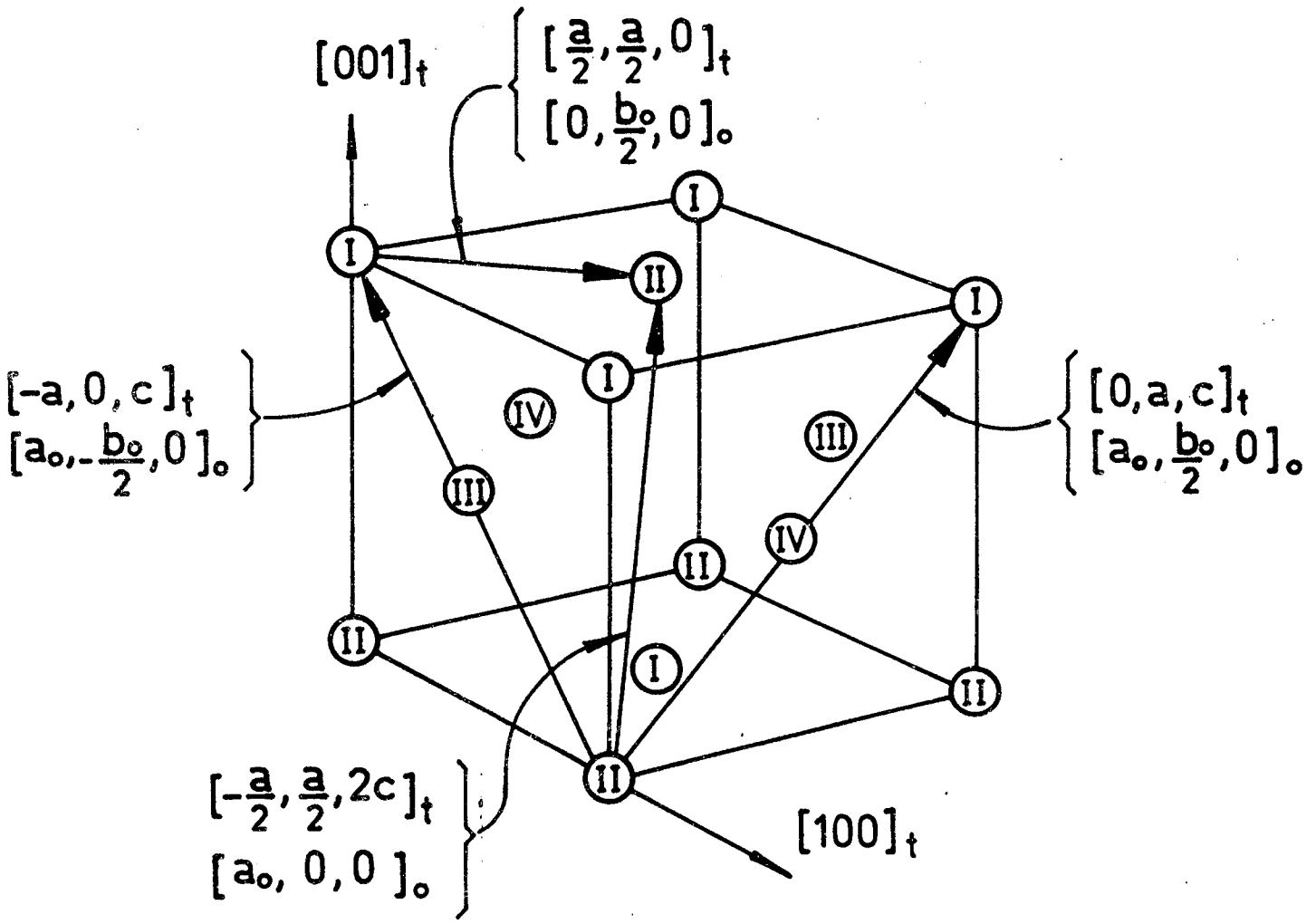
$[001]_t$
$[\frac{a}{2},\frac{a}{2},0]_t$
$[0,\frac{b_o}{2},0]_o$
$[-a,0,c]_t$
$[a_o,-\frac{b_o}{2},0]_o$
$[0,a,c]_t$
$[a_o,\frac{b_o}{2},0]_o$
$[-\frac{a}{2},\frac{a}{2},2c]_t$
$[a_o,0,0]_o$
$[100]_t$
I
II
III
IV